Transacylation Kinetics in Fatty Acid and Polyketide Synthases and its Sensitivity to Point Mutations**

Franziska Stegemann[a] and Martin Grininger*[a]

Fatty acid and polyketide synthases (FASs and PKSs) synthesize physiologically and pharmaceutically important products by condensation of acyl building blocks. The transacylation reaction catalyzed by acyl transferases (ATs) is responsible for the selection of acyl-CoA esters for further processing by FASs and PKSs. In this study, the AT domains of different multi-domain (type I) PKS systems are kinetically described in their substrate selectivity, AT–Acyl carrier protein (ACP) domain-domain interaction and enzymatic kinetic properties. We observe that the ATs of modular PKSs, intricate protein complexes occurring in bacteria and responsible for the biosynthesis of bioactive polyketides, are significantly slower than ATs of mammalian FASs, reflecting the respective purpose of the biosynthetic pathways within the organism and their metabolic context. We further perform a mutational study on the kinetics of the AT–ACP interaction in the modular PKS 6-deoxyerythronolide B synthase (DEBS) and find a high plasticity in enzyme properties, which we explain by a high plasticity in AT–ACP recognition. Our study enlarges the understanding of ATs in its molecular properties and is similarly a call for thorough AT-centered PKS engineering strategies.

Introduction

Fatty acid synthases (FASs) and polyketide synthases (PKSs) generate important products of primary and secondary metabolism. Palmitic and stearic acid are the main products of FASs and serve a multitude of cellular functions.[1] Polyketides are secondary metabolites of elaborate chemistry and of high bioactivity[2] of which several are harnessed for therapeutic treatment; e.g. as antibiotic (erythromycin, pikromycin, chlorothricine), immunosuppressant (rapamycin) or antineoplastic (epothilone) agent.[3] Despite the fact that they are chemically different and involved in different cellular functions, fatty acids and polyketides share a common biosynthetic origin.

Fatty acids and polyketides are assembled from small building blocks, the acyl-CoA ester substrates, which are loaded and processed during biosynthesis. FASs and PKSs occur as type II systems in which every catalytic function is provided by a separate protein and as type I systems in which the enzymatic functions are harbored on one or several polypeptide chains.[4] FASs and PKSs consist of one distinct set of protein folds whether they occur as separate enzymes or as enzymatic domains. In this study, the focus is on type I systems, which are the predominant systems in eukaryotic *de novo* fatty acid synthesis and responsible for the synthesis of the plethora of elaborate polyketides. The terms FAS and PKS will refer to type I FAS and type I PKS in the following.

FASs and a subset of PKS systems – the iterative PKSs – use one set of catalytic domains harbored on one protein complex in repeating synthetic cycles. While FASs strictly reduce the growing chain fully in every cycle, iterative PKSs generally run non-reductive cycles in which a catalytic step of one of the cycles may be omitted, a property termed cryptic coding.[5–7] In contrast, modular PKSs harbor several sets of catalytic domains, organized in so-called modules, of which each is responsible for incorporation of one extender unit. A PKS module is comprised by a minimum of three catalytic domains that are all required for the elongation of the growing acyl chain with the extender unit: β-ketoacyl synthase (KS), acyl transferase (AT) and acyl carrier protein (ACP). Processing functions can enlarge this minimal set provided by domains: β-ketoacyl reductase (KR), dehydratase (DH) and β-enoyl reductase (ER) (Figure 1A). In running vectorial synthesis and varying the enzymatic repertoire module by module, modular PKSs harness the synthetic capacity of this protein family in diametrically different manner to FASs and iterative PKSs (Figure 1B).[8,9]

In this study, we characterize ATs of three different modular PKSs and one iterative PKS and compare this data with the AT of the mammalian FAS (termed MAT) (Figure 2 and Figure S1). Specifically, we report enzyme kinetic constants of those AT domains and describe similarities and differences in the transacylation reaction in the context of the cellular function of the entire protein. Our data proposes that ATs of PKSs are in general slower than of FASs, which well reflects the different purpose of the biosynthetic pathways. Whereas fatty acids are essential compounds of all living entities (except archaea) and needed in high amounts, polyketides are secondary metabolites

[a] F. Stegemann, Dr. M. Grininger
Institute of Organic Chemistry and Chemical Biology
Buchmann Institute for Molecular Life Sciences
Goethe University Frankfurt
Max-von-Laue-Str. 15
60438 Frankfurt am Main (Germany)
E-mail: grininger@chemie.uni-frankfurt.de

[**] A previous version of this manuscript has been deposited on a preprint server (https://doi.org/10.1101/2020.12.29.424742).

Supporting information for this article is available on the WWW under https://doi.org/10.1002/cctc.202002077

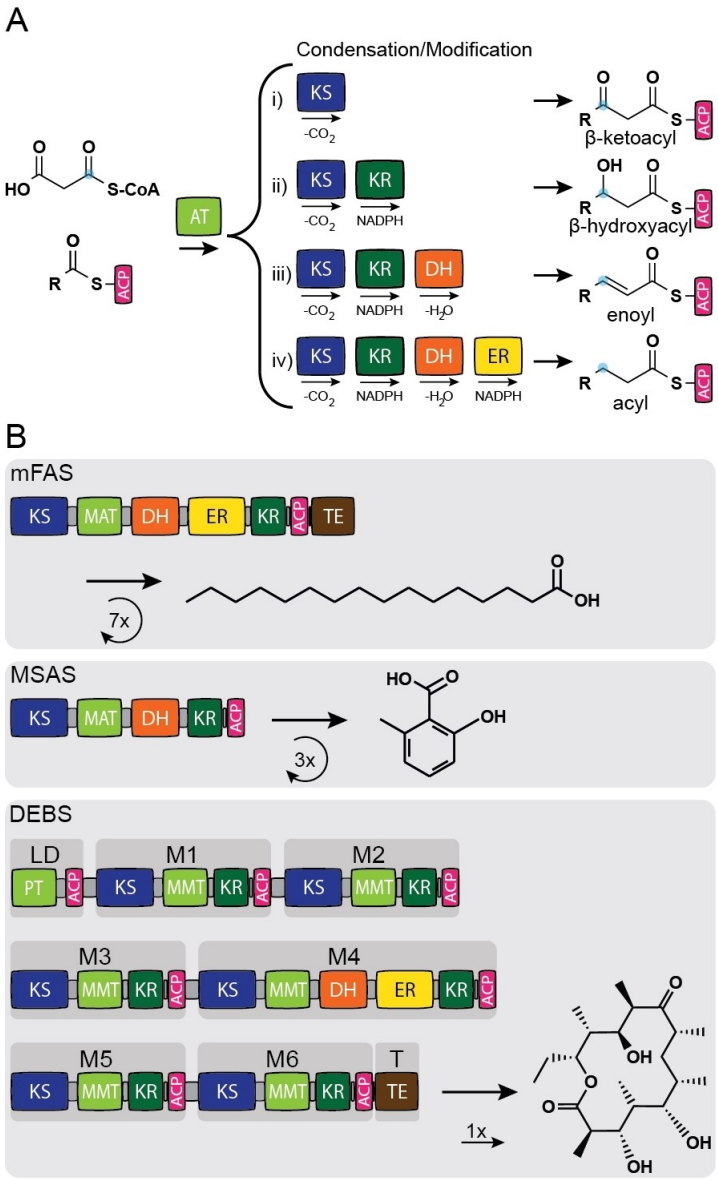

Figure 1. Synthesis of fatty acids and polyketides. (A) Module composition of PKSs: The minimal PKS module (i) consists of domains KS, AT and ACP leading to a β-ketoacyl product and can be modified by the processing domains KR, DH and ER leading to β-hydroxyacyl (ii), enoyl (iii) or acyl (iv) products. "R" is referring to an alkyl chain from either the priming substrate or the growing chain. FASs contain a full set of domains leading to fully saturated fatty acids. (B) FASs, like the murine FAS (mFAS) and iterative PKSs, like the 6-methylsalicylic acid synthase (MSAS), use their domains several times during synthesis. Modular PKSs, like 6-deoxyerythronolide B synthase (DEBS), follow an assembly line-like synthesis in which each domain is only used once during synthesis and the growing polyketide chain is passed from one module to another. Abbreviations: PT: propionyl transferase, MAT: malonyl/acetyl transferase, MMT: methylmalonyl transferase, TE: thioesterase, LD: loading module, M1–M6: module 1–6, T: termination module.

that can take effect at low concentrations. Further, employing module 5 of the modular PKS 6-deoxyerythronolide B synthase (DEBS M5) as a testbed, we reveal the high sensitivity of the transacylation reaction towards AT:ACP interface mutations, which we trace back to the plasticity in the AT–ACP interplay, recently proposed for type II FAS.[10] Particularly, the surface amino acid R850 of DEBS M5 is a hot spot in this regard. These findings are important for PKS engineering, as disclosing both constraints and possibilities in AT-centered engineering strategies.

Results and Discussion

Kinetic analysis of AT-mediated reactions

The AT domain catalyzes the transfer of the acyl moiety X of the substrate X–coenzyme A (X–CoA) onto the *holo*-ACP domain (Figure 3). The transacylation reaction follows a double displacement mechanism, called ping-pong bi-bi mechanism.[13] The ping step denotes the first transfer of the acyl moiety X onto the AT, resulting in release of product CoA. The pong step denotes the second transfer of the acyl moiety X onto the ACP

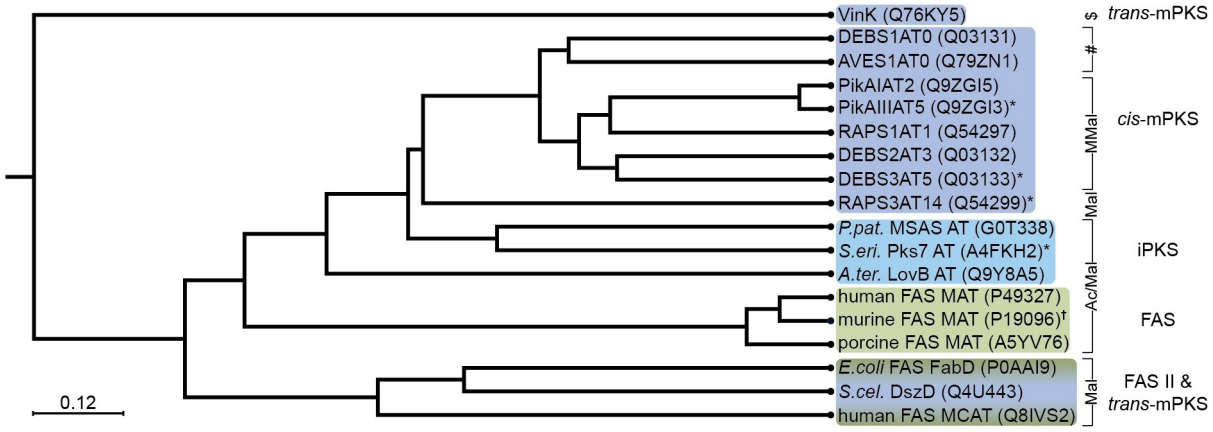

Figure 2. Schematic representation of the phylogenetic relationship between AT domains from FASs and PKSs. ATs from modular PKSs form a distinct clade with a subclade for the loading ATs (# indicates priming substrates: propionyl–CoA for DEBS1 AT0 and 2-methylbutyryl–CoA for AVES1 AT0). As expected, RAPS3 AT14 accepting malonyl (Mal) is separated from the methylmalonyl (MMal) transferring ATs. ATs from iterative PKSs fall into a distinct clade. FAS II ATs form a distinct clade with the *trans*-acting AT DszD from disorazole PKS. All three ATs transfer Mal as substrate. The *trans*-acting AT VinK from vicenistatin PKS transfers an unusual substrate – a dipeptidyl moiety (indicated by $)[11] – and falls into a different clade. FAS systems depicted in green (type I light green, type II dark green), iterative and modular PKS systems (iPKS and mPKS) shown in blue and violet, respectively. ATs analyzed in this study are indicated by *. The MAT analyzed in a previous study and discussed in this study is marked with †.[12] Phylogenetic tree created using CLC Main Workbench 6.9.1 (tree construction method: UPGMA, protein distance measure: Jukes-Cantor, bootstrap value = 100).

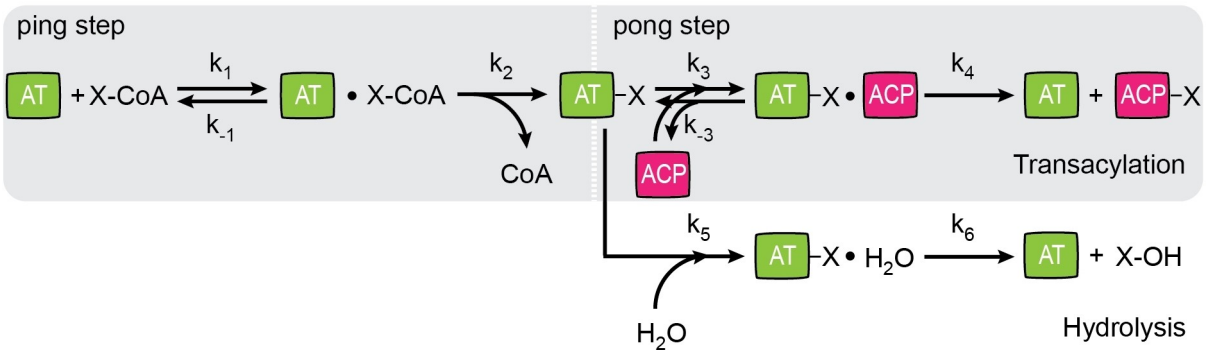

Figure 3. Schematic representation of AT-mediated reactions. After formation of the enzyme (AT)-substrate (X–CoA) complex, free CoA is released and AT–X is formed. The substrate X is either transacylated via formation of the enzyme (AT–X)-substrate (ACP) complex (main branch) or hydrolyzed during AT-mediated hydrolysis (side branch). Kinetic constants k_1 to k_6 describe the AT-mediated reactions.

after binding of the second substrate ACP to AT–X, leading to the final product ACP–X. Hydrolysis occurs as side reaction, releasing the free acid "X–OH". To quantify transferase activity, an enzyme-coupled, fluorescence-based assay was established, based on previous work.[12,14,15] Kinetic parameters (Figure S2) were determined for both AT-mediated transacylation and AT-mediated hydrolysis. For the mathematical description, see Supporting Information Note 1.

To understand similarities and differences between types of FASs and PKSs, the following AT domains were selected for analysis in this study: Representing the AT domain of modular PKSs, the AT of DEBS M5 from *Saccharopolyspora erythraea* (termed DEBS3M5), of pikromycin synthase (PikA) M5 from *Streptomyces venezuelae* (PikAIIIM5) and of rapamycin synthase (RAPS) module 14 from *Streptomyces hygroscopicus* (RAPS3M14) were used. The first two AT domains transfer methylmalonyl (MMal), while the latter transfers malonyl (Mal).[2,16] For the iterative PKSs, we worked with the AT domain of Pks7 found in *S. erythraea*. Pks7 AT is phylogenetically similar to 6-methylsalicylic acid synthase (MSAS) AT from *Penicillium patulum* and is likely involved in methylsalicylic acid (MSA) synthesis (Figure 2).[17] Data will be compared to the previously analyzed murine FAS (mFAS), which was found to be promiscuous in transferring a large variety of substrates.[12] The AT domain of Pks7 is expected to load acetyl (Ac) and Mal onto the ACP domain for MSA production.[3,7,18] The specificity for Mal, and not MMal, is supported by the amino acid fingerprint of Pks7 AT.[3]

Recent functional and structural characterization revealed that FAS and PKS systems form stable KS-AT dimers.[12,19] Therefore, all AT domains used in this study were expressed as KS-AT didomains. A KS knockout, leading to constructs denoted as KS^0-AT, allowed for selectively inspecting the AT domain in transacylation properties. Recombinant expression of KS^0-ATs and standalone ACPs in *E. coli* gave sufficient yields of soluble,

high-quality proteins (Table S1–S4 and Figure S3–S7). We performed a substrate screen on AT domains with Ac, Mal and MMal that basically confirmed the substrate specificity of the AT domains (Table S5 and Figure S8). Like reported before,[15,20] most AT domains hydrolyze their native substrates with higher rates than non-native substrates, confirming that there is no general hydrolysis-based proofreading mechanism represented in AT domains. Only PikAIII AT5 did show higher hydrolysis rates for the non-native extender substrate Mal, which was also reported for PikAIV AT6.[21] Please find further details in Supporting Information Note 2. Based on this initial screening, full kinetic analysis of AT-mediated hydrolysis and transacylation was performed with the substrates that are preferentially transferred.

Kinetic characterization of hydrolysis

To analyze AT-mediated hydrolysis, the substrates X–CoA were titrated in absence of ACP. We faced difficulties in conducting the hydrolysis assay, originating from extreme differences in K_m^{X-CoA}, and we would like to refer to the Supporting Information Note 3 for more information. Only DEBS3M5 AT-mediated hydrolysis was eventually characterized in K_m^{X-CoA} and k_{cat} at high confidence, while for the other AT domains of PKSs partly just rough values were determined (Table 1). The kinetic parameters for DEBS3M5 AT-mediated hydrolysis are very similar to the data for DEBS2M3 AT-mediated hydrolysis previously published by Dunn *et al.*[15] Overall, AT-mediated hydrolysis rates for the native substrates are similar for all analyzed PKS systems. Hydrolysis mediated by the MAT domain of mFAS (termed mMAT) is very slow compared to the PKS systems. For hydrolysis titration curves, see Figure S9.

Kinetic characterization of transacylation

To characterize the transacylation reaction, both substrates X–CoA and ACP were titrated. Specifically, we titrated X–CoA substrates to five different, fixed ACP concentrations and globally fitted all titration curves. This approach is robust to measurement errors as well as delivers absolute kinetic constants and is in its quality superior to other approaches titrating one substrate while keeping the other at a fixed saturated concentration.[22,23] For all ATs, absolute kinetic parameters were received, although the kinetic parameters for systems with high K_m^{ACP} were determined less accurately, simply because the vast amounts of ACP needed to cover an appropriate substrate range could not always be provided. This was particularly problematic for Pks7. Here, the ACP concentration was varied only within a range of 0.16–0.80 × K_m^{ACP} for the substrate MMal–CoA.

Overall, data reveals that PKS systems feature slower turnover rates than found in AT of FAS type I (and type II) (Table 2 and Figure 4),[12,23,24] with the AT domain of the iterative Pks7 transferring the substrates with significantly higher rates than AT domains of modular PKSs. Catalytic efficiencies k_{cat}/K_m^{X-CoA} and k_{cat}/K_m^{ACP} show that the mMAT transacylates with highest efficiency, followed by the iterative Pks7 AT (about one order of magnitude less efficient than mMAT) and modular PKSs (another order of magnitude less efficient than Pks7 AT), indicating that the iterative systems feature low transition state energies for the transacylation reaction. Particularly, the catalytic efficiencies of the AT-acylating ping step k_{cat}/K_m^{X-CoA} is outstandingly high for mMAT compared to ATs of modular PKSs; e.g., Mal is transferred by mMAT with catalytic efficiency of $8.3\times10^6\ M^{-1}s^{-1}$ compared to RAPS3 AT14 with $4.8\times10^4\ M^{-1}s^{-1}$ (Table 2).

Comparing the AT loading (ping) step with the ACP loading (pong) step in catalytic efficiencies by forming the ratio $\left(k_{cat}/K_m^{X-CoA}\right)/\left(k_{cat}/K_m^{ACP}\right)$ shows that the iterative systems feature

Table 1. Kinetic parameters determined for AT-mediated hydrolysis. Abbreviations: n.d.: not determinable.

Protein X–CoA	k_{cat} (s^{-1})	K_m^{X-CoA} (μM)	k_{cat}/K_m^{X-CoA} ($M^{-1}s^{-1}$)
DEBS3AT5 MMal	$5.31\times10^{-2}\pm9.62\times10^{-4}$	$7.88\pm3.98\times10^{-1}$	6.7×10^3
PikAIIIAT5 MMal [a]	$1.94\times10^{-2}\pm5.03\times10^{-4}$	$<8.91\times10^{-1}$	$>2.2\times10^4$
PikAIIIAT5 Mal [b]	*$1.95\times10^{-1}\pm1.54\times10^{-2}$*	*99.9 ± 28.8*	n.d.
RAPS3AT14 Mal [a]	$6.51\times10^{-2}\pm1.89\times10^{-3}$	$<5.45\times10^{-1}$	$>1.2\times10^5$
Pks7 AT Mal [a]	$9.93\times10^{-2}\pm3.17\times10^{-3}$	$<4.74\times10^{-1}$	$>2.1\times10^5$
Pks7 AT MMal [a]	$7.34\times10^{-2}\pm1.51\times10^{-3}$	$<3.98\times10^{-1}$	$>1.8\times10^5$
mMAT Mal [c]	$(9.8\pm1.7)\times10^{-3}$	n.d.	n.d.
mMAT MMal [c]	$(6.0\pm1.2)\times10^{-3}$	n.d.	n.d.
mMAT Ac [c]	$9.3\times10^{-3}\pm1.2\times10^{-4}$	n.d.	n.d.

[a] This system has a very low K_m^{X-CoA}. Only k_{cat} is determined precisely. [b] This system has a very high K_m^{X-CoA}. Measurement gave large signal fluctuations (Figure S8). Corresponding kinetic values with substantial errors are indicated by constants in italic letters. [c] mMAT data from previous study.[12]

Table 2. Kinetic parameters determined for transacylation.

Protein X–CoA	k_{cat} (s^{-1})	K_m^{X-CoA} (μM)	K_m^{ACP} (μM)	k_{cat}/K_m^{X-CoA} ($M^{-1}s^{-1}$)	k_{cat}/K_m^{ACP} (M^{-1s-1})	k_{cat} norm (%)	k_{cat}/K_m^{X-CoA} norm (%)	k_{cat}/K_m^{ACP} norm (%)	k_{cat}/K_m^{X-CoA} / (k_{cat}/K_m^{ACP})
DEBS3 AT5 MMal	$1.25 \pm 7.11 \times 10^{-2}$	209 ± 17.5	72.0 ± 8.21	6.0×10^3	1.7×10^4	1.1	4.3×10^{-2}	3.5	3.4×10^{-1}
PikAIII AT5 MMal	$7.47 \pm 5.16 \times 10^{-1}$	96.2 ± 8.69	330 ± 44.1	7.8×10^4	2.2×10^4	6.3	5.6×10^{-1}	4.5	3.4
RAPS3 AT14 Mal	$7.10 \times 10^{-1} \pm 3.84 \times 10^{-2}$	14.8 ± 1.33	66.0 ± 10.8	4.8×10^4	1.1×10^4	6.0×10^{-1}	3.4×10^{-1}	2.2	4.6
Pks7 AT Mal	23.4 ± 1.50	$9.48 \pm 8.84 \times 10^{-1}$	286 ± 30.3	2.5×10^6	8.2×10^4	20	18	17	30
Pks7 AT MMal	20.5 ± 2.03	21.1 ± 2.46	505 ± 73.8	9.7×10^5	4.1×10^4	17	6.9	8.4	24
mMAT Mal [a]	119	8.8	245	1.4×10^7	4.9×10^5	100	100	100	28
mMAT Ac [a]	99.2	12	265	8.3×10^6	3.7×10^5	83	59	76	22

[a] mMAT data from previous study.[12]

efficiency ratios of up to 30 for native extender substrates, while ratios for the slower modular PKS systems are significantly lower (Table 2). We interpret a high ratio as representing an AT domain that is particularly efficient in the initial acylation ping step (AT–X formation) and, in doing so, supports high overall transacylation rates due to a higher probability of a productive AT–X–ACP interaction in the pong step. Following this interpretation, the high catalytic efficiency of Pks7 AT and mMAT in their ping step is key to overall high turnover rates. Vice versa, the lower efficiency in the ping step of ATs of modular PKSs contributes to their slower transacylation rates.

The K_m^{X-CoA} values for Ac–CoA and Mal–CoA are in the range of bacterial metabolite levels[25] and are similar for most AT substrate pairs. Interestingly, the $K_m^{MMal-CoA}$ (K_m^{X-CoA} for MMal–CoA) values for DEBS3 AT5 and PikAIII AT5 are 10 to 20-fold higher than K_m^{X-CoA} for other systems tested (Table 2). This either indicates an adaptation to higher cellular MMal–CoA levels or a control mechanism for regulating MMal uptake depending on its availability. The regulation of polyketide biosynthesis by AT-mediated transacylation would be particularly efficient, when a limited metabolic flux of MMal into the polyketide biosynthetic pathway upon shortage of MMal–CoA (possible by the high $K_m^{MMal-CoA}$) becomes overall rate limiting. We note that a similar regulation of polyketide biosynthesis would not be plausible with Mal–CoA, which is dedicated mainly to the central metabolism of any bacterial cell and regulated in concentration to its need as precursor in fatty acid biosynthesis.[26]

Our data further shows that Michaelis-Menten constants K_m^{ACP} vary moderately for the different ATs (Table 2). Considering molar concentrations within the FAS/PKS compartment of about 1 mM (rough calculation based on a cylinder volume of dimensions taken from mycocerosic acid synthase (MAS)-like PKS; i.e., radius 10 nm, height 15 nm; 2 molecules) as well as freely diffusing domains within the multidomain compartment, all AT domains of type I systems operate at high (Pks7) to saturated (other systems tested) ACP conditions so that the pong step runs at maximum rate (v_{max}).

The analysis of the AT domain of the iterative Pks7 in transferring Mal and MMal gives further interesting insight into the AT-mediated transacylation. Both Michaelis-Menten constants K_m^{X-CoA} and K_m^{ACP} differ for the two tested extender substrates Mal–CoA and MMal–CoA (Table 2), which implies that the interaction of AT and ACP is modulated by the substrate to be transferred, similarly as recently suggested for *E. coli* type II FAS.[23] Catalytic efficiencies differ for the two substrates, indicating a higher efficiency for Mal in both steps, the AT loading ping and the ACP loading pong step. This data suggests a double selection for the native Mal over the non-native MMal to ensure the specific condensation with Mal. For transacylation titration curves, see Figure S10.

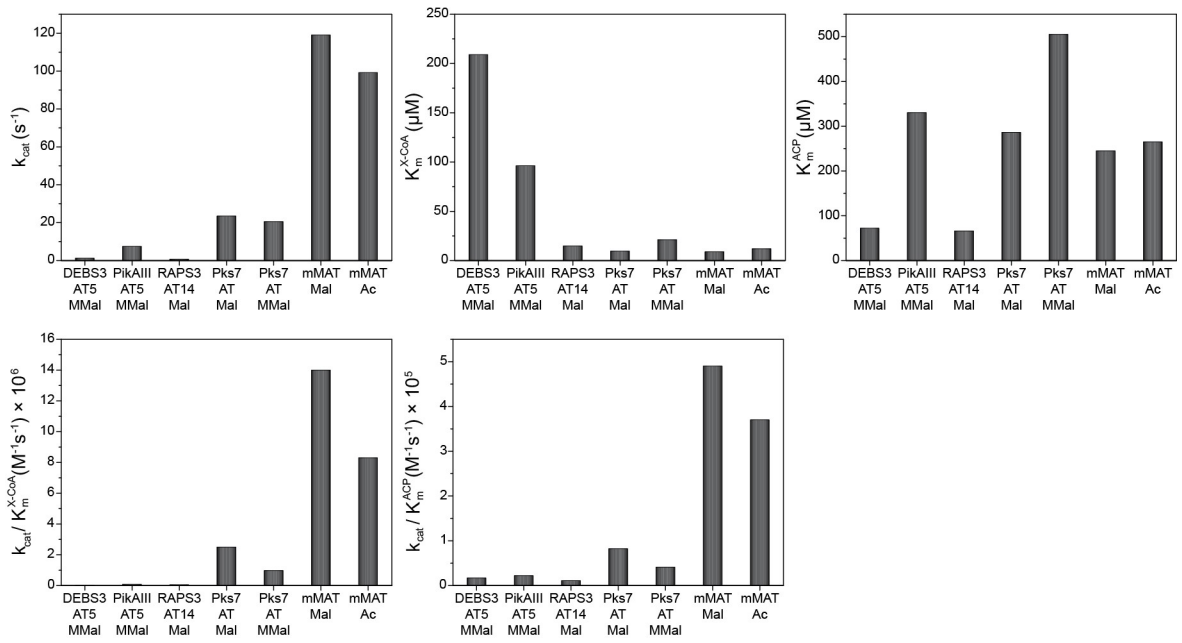

Figure 4. Turnover rate, Michaelis-Menten constants and catalytic efficiencies determined for transacylation for the FAS and PKS systems. mMAT data from previous study.[12]

Implications on the AT mechanism by comparing hydrolysis and transacylation

Our enzyme kinetic analysis reveals that hydrolysis mediated by ATs of PKS systems is just one to two orders of magnitude slower than transacylation, which is in accordance with previous studies.[15,20] This rate difference is much less than for FAS systems for which four orders of magnitude difference were recorded.[12] We observe AT-mediated hydrolytic activity for all substrates – if native or non-native – transferred onto the ACP during transacylation and in most cases hydrolysis is fastest for the native substrates (Figure S8). The purpose of the relatively high hydrolysis rates for PKSs remains elusive, but our data rules out any quality control by hydrolysis, as e.g. reported for some aminoacyl-tRNA synthetases in which hydrolytic active sites evolved in addition to their catalytic active sites.[27]

Comparing AT-mediated transacylation and AT-mediated hydrolysis can give insight in the substrate specificity of enzymes. (i) The PikAIII AT5 is the only enzyme from our set of proteins for which we recorded a higher hydrolysis rate for the non-native substrate, although at low rate speaking also in the specific case of PikAIII AT5 against a proofreading function. Different specificities for hydrolysis and transacylation are interesting from a mechanistic point of view, because they can just arise after the substrates have been loaded to the enzyme (after the ping step). Data implies that PikAIII AT5 can forward the native moiety MMal to the ACP loading pong step, while redirecting the non-native moiety Mal into hydrolysis. In this regard, PikAIII AT5 seems capable of differentiating between the two substrates in the pong step. (ii) In case of the other modular PKSs (DEBS3M5 and RAPS3M14), the absence of hydrolytic activity for non-native substrates, with respect to the detection limit of our assay, indicates a more stringent selection for substrates in the ping step. (iii) We note that, based on the catalytic efficiency of the ping step, we can calculate the Michaelis-Menten constants for the AT-mediated hydrolysis (Table S6). This is possible, because the efficiencies for the ping step in transacylation and for hydrolysis are identical (Figure S2). We observe decreasing K_m^{X-CoA} values for hydrolysis from modular PKSs to the iterative PKS to the FAS system. This trend, as well as the trend in catalytic efficiencies (increased for iterative proteins), is overall similar to the ping step of transacylation.

Implications on FAS/PKS function and evolution

Bar-Even and Noor *et al.*[28] have mined enzyme databases for a systematic study on kinetic parameters of enzymes and substrates. As one of their key findings, they revealed that enzyme substrate pairs associated with primary metabolism tend to have higher turnover numbers than pairs of secondary metabolism and also average k_{cat}/K_m values are higher in primary than in secondary metabolism. We observe a very similar trend in our study on the transacylation function in FASs and PKSs; i.e., high turnover rates by MAT of FASs[12,29] and low turnover rates by ATs of modular PKSs. The lower turnover rates and catalytic efficiencies can be explained by serving the purpose of PKSs in providing sufficient efficiency to produce molecules at a low basal level or when necessary without draining vital metabolic pools (particularly in case of using Mal–CoA as extender substrate). In contrast, the MAT domain of FAS needs to be fast and was under selection pressure for providing high rates for the high metabolic fluxes that are

required by the central metabolic fatty acid biosynthesis. In conclusion, we observe in our dataset that the AT domains have evolved differently, serving the different purposes in enzyme function in the metabolic context.[30]

In previous studies, the lab of Stuart Smith and we described MAT from rat and mouse FAS as fast, substrate polyspecific and plastic,[12,29,31] which are typical properties of primordial enzymes. We speculate that in MAT primordial enzyme properties kept preserved due to its role in fatty acid synthesis and due to the KS-mediated condensation step ensuring the fidelity of the fatty acid biosynthesis.[31] Compared to MAT of FAS, the ATs of modular PKSs appear more specialized. Although ATs of modular PKSs with substrate tolerance towards mainly non-native elongation substrates have been reported,[20,21,32,33] they have the ability to selectively transfer the native elongation substrates Mal and MMal, as we show in this study. Here, we note that we have not tested the transacylation of the native substrate ethylmalonyl–CoA.

Given that AT domains are integral part of mono-modular iterative PKSs and modules of modular PKSs, their course of evolution is likely closely connected to the evolution of PKSs in general. Current models on the evolution of PKSs consider modular PKSs as successors of simpler systems that have likely been (also) iterative PKSs (and FASs or their precursor).[34–38] Accordingly, it is tempting to speculate that a primordial AT enzyme, to which MAT of FAS is still reminiscent in functional properties, has developed into more selective and slower modular AT domains (as they appear from the dataset of this study) as part of PKS evolution.

AT:ACP interface mutation study

Some of the molecular details to the ACP-mediated shuttling of substrates and intermediates to the catalytic domains in FASs and PKSs are being currently revealed. For example, interactions are guided by weak electrostatic interactions,[39] and, as shown for the AT–ACP interaction in the *E. coli* type II system (FabD:AcpP interface), do not necessarily involve prevalent interfaces.[10] In order to help understanding this critical domain–domain interaction in type I complexes, the AT:ACP interface of DEBS3M5 was mutated and analyzed with the transacylation assay in enzyme kinetic detail. Three available AT:ACP complex structures[11,40,41] were used for selecting interface mutations (Figure S11). Eventually two residues, A539 and R850, were selected that are likely involved in the AT–ACP interaction. Overall, nine point mutations were introduced in the AT domain of the KS^0-AT didomain construct of DEBS3M5; A539S, A539D, A539E, A539F, R850K, R850A, R850E, R850F, R850S. All mutants showed wild type-like properties during preparation (Table S7–S8 and Figure S12–S14).

In an initial screen, the mutants were tested in transacylation activity at fixed MMal–CoA and fixed ACP concentrations. We additionally screened the hydrolysis rates at fixed MMal–CoA concentrations. Since AT-mediated hydrolysis does not involve ACP, hydrolysis rates are able to report any non-local effect of the surface mutation. Our initial screen revealed that some mutations affect both transacylation and hydrolysis, although the impact on hydrolysis was comparably lower than on transacylation (Figure 5). This data shows that indeed some surface point mutations are invasive to structural and conformational properties that determine the enzymatic reaction. This phenomenon was pronounced for mutations introduced at R850, and not for A539, as depicted in Figure 5.

Based on the initial screening, four mutations were chosen for full kinetic characterization to determine absolute kinetic constants; i.e., A539E, which shows nearly no effect in screening, and the mutations R850K, R850E and R850S, which show moderate to strong effects, preserving, inverting and neutralizing the charge of the mutated residue. For protein quality control of proteins in biological replicates, see Table S8 and Figures S12–S14. The ACP concentrations for the enzymatic analysis of mutant R850E were within a non-ideal range of 1–$22\times K_m^{ACP}$ due to a low K_m^{ACP} value and the kinetic transacylation parameters for this mutant could just be determined at lower confidence.

Transacylation and hydrolysis turnover rates well reflect the initial screening (Table 3 and Figure 6, for hydrolysis and transacylation titration curves, see Figure S15 and S16). Mutant A539E showed comparable transacylation rates to the wild type protein (82% of wild type). Overall, kinetic characterization indicates that the site A539 is rather not involved in the AT–ACP and the AT–MMal–CoA interaction or mutations are not invasive to the AT–ACP interaction. The kinetics of the transacylation reaction is essentially unaltered compared to the wild type, as can also be seen in transition state energies for the ping step and pong step remaining at wild type level (Figure 7). In contrast, R850 mutants were significantly compromised in transacylation activity (R850K with 57% of wild type, R850E 5.5% and R850S 23%). Hydrolysis rates remained unaltered by

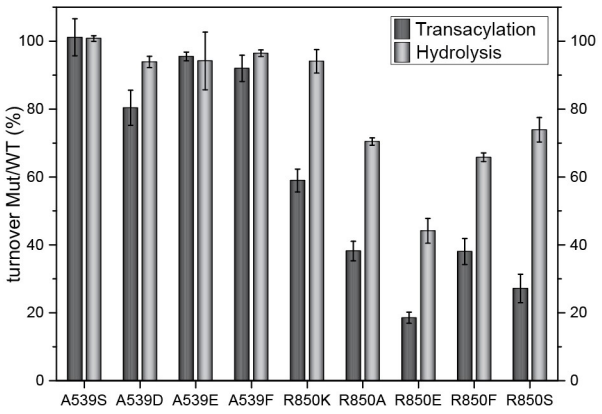

Figure 5. Transacylation (dark grey) and hydrolysis (light grey) screening of the different DEBS3M5 AT:ACP point mutants. The transacylation activity is measured in technical triplicates of one biological replicate; hydrolysis is measured in biological (A539E, R850K, R850E, R850S) or technical triplicates (A539S, A539D, A539F, R850A, R850F). The average activity of each mutant (Mut) is divided by wild type's (WT) activity and is given in %. Error bars indicate the standard deviation of technical or biological triplicates. A539 mutants seem to have no influence on transacylation and hydrolysis, whereas R850 mutants decrease both transacylation and hydrolysis rates significantly.

Table 3. Transacylation and hydrolysis kinetic parameters determined for DEBS3AT5 wild type and mutants with MMal–CoA. For hydrolysis and transacylation titration curves of all mutants, see Figure S15 and S16. Overall, transacylation and hydrolysis kinetic parameters are in good accordance and the catalytic efficiencies give similar values for each mutant, as it should be. No mutation is wild type AT (DEBS3AT5 WT).

Transacylation						Hydrolysis		
Mutation	k_{cat} (s^{-1})	$K_m^{MMal-CoA}$ (μM)	K_m^{ACP} (μM)	$k_{cat}/K_m^{MMal-CoA}$ ($M^{-1}s^{-1}$)	k_{cat}/K_m^{ACP} ($M^{-1}s^{-1}$)	k_{cat} (s^{-1})	$K_m^{MMal-CoA}$ (μM)	$k_{cat}/K_m^{MMal-CoA}$ ($M^{-1}s^{-1}$)
–	$1.25 \pm 7.11 \times 10^{-2}$	209 ± 17.5	72.0 ± 8.21	6.0×10^3	1.7×10^4	$5.31 \times 10^{-2} \pm 9.62 \times 10^{-4}$	$7.88 \pm 3.98 \times 10^{-1}$	6.7×10^3
A539E	$1.02 \pm 5.19 \times 10^{-2}$	164 ± 13.5	74.3 ± 7.96	6.2×10^3	1.4×10^4	$5.16 \times 10^{-2} \pm 1.15 \times 10^{-3}$	$9.99 \pm 6.06 \times 10^{-1}$	5.2×10^3
R850K	$7.10 \times 10^{-1} \pm 5.82 \times 10^{-2}$	121 ± 16.3	73.2 ± 12.7	5.9×10^3	9.7×10^3	$5.38 \times 10^{-2} \pm 1.59 \times 10^{-3}$	$11.2 \pm 8.75 \times 10^{-1}$	4.8×10^3
R850E	$6.82 \times 10^{-2} \pm 3.04 \times 10^{-3}$	75.5 ± 7.65	2.38 ± 0.408	9.0×10^2	2.9×10^4	$3.59 \times 10^{-2} \pm 1.79 \times 10^{-3}$	37.7 ± 5.37	9.5×10^2
R850S	$2.82 \times 10^{-1} \pm 1.41 \times 10^{-2}$	140 ± 11.7	46.0 ± 4.55	2.0×10^3	6.1×10^3	$5.32 \times 10^{-2} \pm 2.94 \times 10^{-3}$	25.9 ± 3.60	2.1×10^3

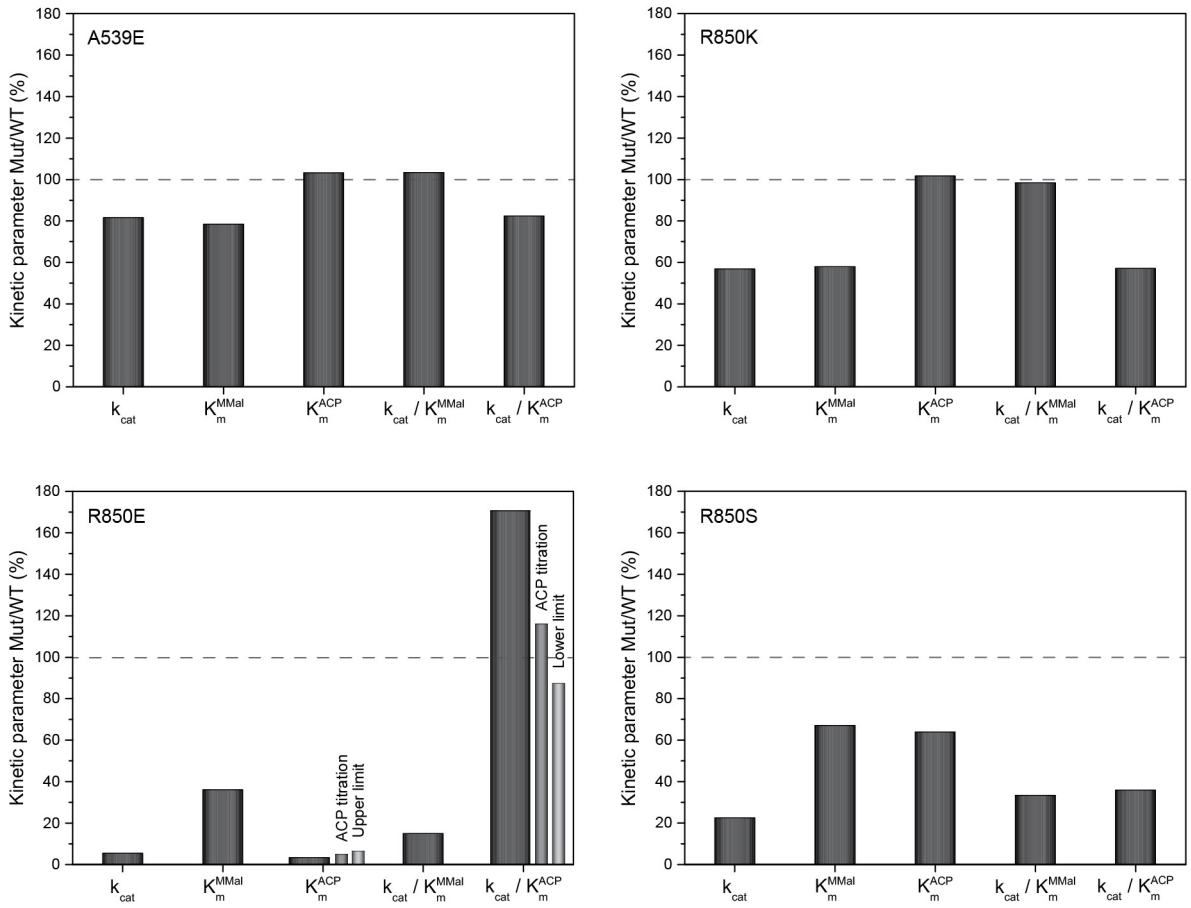

Figure 6. Ratio of kinetic constants determined for transacylation catalyzed by mutants (Mut) A539E, R850K, R850E and R850S and wild type DEBS3M5 AT (WT) kinetic constants in %. R850E shows three ratios of K_m^{ACP} Mut/WT corresponding to the different K_m^{ACP} received for this mutant: value determined via global fit (ratio shown in dark grey), determined via ACP titration without lowest ACP concentration (ratio shown in grey) and the upper limit of the value (ratio shown in light grey). Accordingly, this gives three corresponding ratios for the catalytic efficiency k_{cat}/K_m^{ACP}.

the mutations A539E, R850K and R850S, but dropped to 68% of wild type rates for mutation R850E. We note (again) that the transacylation rate always includes the hydrolysis rate to some extent.

Impact of interface mutations on transacylation kinetics

In contrast to A539E, mutations in R850 led to intricate effects on both the AT loading ping and the ACP loading pong step. (i) The mutation R850K, preserving the positive charge, has almost no influence on the AT–MMal–CoA interaction, as indicated by the ping step remaining unaltered in catalytic efficiency and transition state energy compared to wild type DEBS3M5 AT (Figure 7). However, the pong step drops in efficiency and overall reduces turnover rates for transacylation (57% of wild type). The K_m^{ACP} of the pong step is similar to wild type AT, which indicates unchanged AT–X:ACP complex stability. Since the catalytic rate of the pong step (k_4) is decreased, K_m^{ACP} can just remain at wild type level when compensated by an increase of

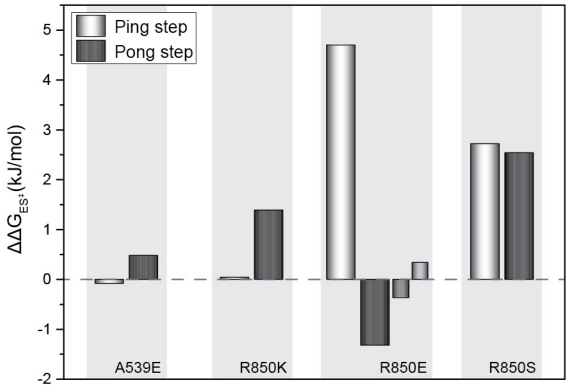

Figure 7. Difference in transition state energy (kJ/mol) between mutants A539E, R850K, R850E and R850S and wild type determined for the ping step (white bars) and the pong step (grey bars) of transacylation. Mutant R850E gives three values for K_m^{ACP}: one determined via global fit, one via ACP titration (grey) and one upper limit (light grey). Differences in transition state energy to wild type are shown in dark grey, grey and light grey, respectively. $\Delta\Delta G_{ES^*} = -RT\ ln\left[\frac{(k_{cat}/K_m)^{Mut}}{(k_{cat}/K_m)^{WT}}\right]$ with the gas constant R, T = 298 K and the ratio of catalytic efficiencies between mutant (Mut) and wild type (WT).

ratio k_{-3}/k_3, indicating that the main effect of the mutation R850K is decelerating the formation (k_3) and/or accelerating the (non-productive) dissociation of AT–X:ACP (k_{-3}) (Figure 8). (ii) The mutant R850E inverses the charge from positive to negative and we expected severe changes in the kinetics of the transacylation reaction. Indeed, we observed lowest turnover rates within our set of mutants. We note that the kinetic parameters of the pong step could only be collected with lower confidence due to the low K_m^{ACP}. For a reliable estimate on K_m^{ACP}, we therefore extracted data for saturated substrate MMal–CoA concentration titrated with ACP and receive a K_m^{ACP} of 3.46 μM and an upper boundary of 4.6 μM (Figure S17). Given this data, we conclude that the pong step remains essentially unaltered in catalytic efficiency and transition state energy. In contrast, the ping step is severely affected by this mutation and responsible for the overall decrease of turnover rates. Since the catalytic rate of the ping step (k_2) is contributing to K_m^{ACP}, the drop of K_m^{ACP} is "just" a direct consequence of the slow ping step. Under this assumption, the kinetics of the pong step would be entirely unaffected in spite of exchanging the positively charged arginine with the negatively charged glutamate (Figure 8). In conclusion, this mutant, designed for a severe impact on the domain-domain interplay during the pong step, mainly (or entirely) takes effect on the initial ping step, which demonstrates the intricate effect surface mutations can have. (iii) In the mutant R850S, both ping step and pong step are affected by the amino acid exchange, as indicated by changed catalytic efficiencies and transition state energies compared to wild type DEBS3M5 AT, and effects cumulate to a decrease in turnover rates to 23% compared to wild type. The decrease in the catalytic rates of the ping step (k_2) and the pong step (k_4) accounts for the increased stabilities of the complexes AT:X–CoA and AT–X:ACP (lowered K_m^{X-CoA} and K_m^{ACP} values), but ratios k_{-1}/k_1 and k_{-3}/k_3 may contribute here (Figure 8). Overall, the effect of mutation R850S is not constrained to the pong step, but also invasive to AT–X formation; i.e., not showing the specific properties expected of an AT:ACP interface mutation.

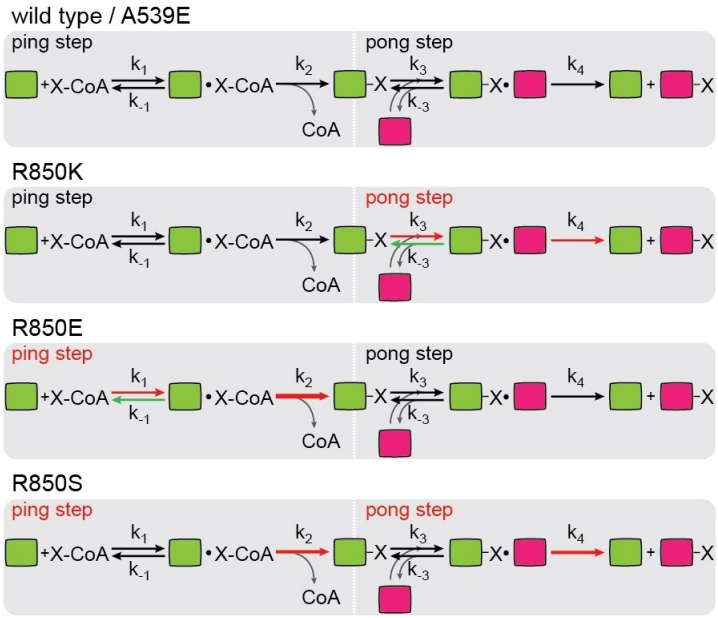

Figure 8. Plasticity of transacylation kinetics. Fluxes through the transacylation pathway in DEBS3M5 AT wild type and mutants. Green and red arrows indicate accelerated and decelerated reactions, respectively. The thicker the arrow, the more pronounced the effect. Only the most probable effects according to our interpretation are shown. Headers "ping step" and "pong step" are in red when decelerated. Domains AT and ACP are depicted as green and pink boxes, respectively.

Implications of interface mutation study on PKS engineering

Electrostatic networks have previously been shown to dominate interactions of ACP with catalytic domains.[23,39] Accordingly, we assumed that R850 with its cationic guanidinium headgroup is likely responsible for a such a key electrostatic interaction at the AT:ACP interface. Further support for R850 being involved in AT–ACP interaction was received from X-ray data in which residue R850 is poorly resolved in electron density in the KS-AT didomain structure (Figure S18),[19] indicating that R850 is not part of an electrostatic network of AT, but involved in AT–ACP interaction. Our kinetic data reflect the importance of the positive charge by the rather moderate effect of R850K mutation on the overall rate of transacylation compared to mutations R850S and R850E erasing and inverting the charge at this amino acid position, respectively. However, with help of the quantitative data, we likewise revealed that the mutations are not constrained to the AT–ACP interplay, but able to change kinetics of the entire transacylation reaction sequence (AT loading ping step and ACP loading pong step).

The incorporation of non-native extender substrates to polyketides has previously been achieved by exchanging AT domains; i.e., replacing the native domain with a domain of interest.[42–44] While such strategies can be successful in delivering the desired compound, the chimeric PKSs inherently suffer from non-cognate (permanent) interfaces in the KS-AT didomain as well as non-cognate (transient) interfaces during substrate shuttling (AT:ACP), which generally leads to compromised activity.[45] Engineering domain-domain interplay can be useful when non-cognate domains are to be integrated in chimeric PKSs. Beyond the boundaries of the DEBS3M5 AT that has served as a model system in this study, the intricate impact of mutations on the catalytic properties suggests that simple engineering strategies based on local effects of amino acid exchanges are prone to fail. For example, engineering interfaces for stabilizing enzyme-substrate complexes (low K_m values) will not necessarily lead to high turnover rates and high catalytic efficiencies. However, the design of chimeric PKSs that perform product synthesis at high efficiency can then be successful, when including detailed enzyme kinetic analysis, ideally complemented by computational methods (as recently demonstrated with FAS[46]) that eventually allows setting up highly effective enzyme kinetic processes.

Conclusion

FASs and PKSs are evolutionary related enzymes. Their AT domains are key players in biosynthesis and responsible for loading acyl substrates onto the ACP domains of the multidomain complexes. Our focused set of AT domains comprises high transacylation rates for ATs of iterative PKSs and FASs of 15 (iterative PKSs) to several hundred molecules per second (FASs) for priming and extender substrates. The tolerance and polyspecificity of ATs of iterative PKSs/FASs towards natural and non-natural substrates was already reported in previous studies.[12,29,47] In contrast, the ATs of modular PKSs appear as significantly decreased in turnover rates (0.7–7 molecules per second) and substrate tolerance, adjusted to their function in selecting the specific elongation substrates for the synthesis of intricate secondary metabolites. Confirming the findings of previous studies, the specificity of AT domains analyzed in this study is in general not assured by hydrolytic proofreading.[15,20]

In addition to a basic characterization of AT kinetic properties, we show that mutations at the interface between AT and ACP can lead to complex kinetic outputs, particularly when affecting the residues involved in the electrostatic network that guides and tunes enzyme–substrate interactions. We show that replacing an arginine, that is likely involved in a key electrostatic interaction at the AT:ACP interface, by lysine, serine or glutamate (R850K, R850S, R850E) leads to a severe drop in enzyme-substrate-complex stability, catalytic efficiencies and turnover rates. The impact of mutations can be explained by changing conformational properties that include those of active site and/or binding tunnel distant to the point mutation. The broadly changing kinetic parameters upon single mutations point towards a plasticity in the interaction of AT with acyl-CoA and ACP, as recently suggested for the AT–ACP interaction in the *E. coli* type II FAS (FabD and AcpP).[10]

Our findings on the kinetic properties of AT domains are highly relevant for AT-centered PKS engineering approaches. Two approaches are essentially possible to achieve the transacylation of an acyl compound of interest: the introduction of specific mutations in the AT binding site, or the swap-in of an entire AT domain natively transferring the compound of interest.[48] Both approaches have been performed successfully (for recent examples, see ref[45,49]). This study can provide guidance in PKS engineering for both of the two approaches: We recommend harnessing the intrinsic specificities of AT-domains from the pool of modular PKSs whenever possible, because those domains will likely provide the required selectivity. In cases where AT domains should be engineered for non-natural extender substrates, the promiscuous ATs of iterative systems may be better suited. Particularly, the MAT domain of the mammalian FAS seems ideal for such approaches, as it appears in functional properties and phylogeny as evolutionary close to a FAS/PKS common ancestor. As a primordial-like enzyme, it can be regarded as better suited to acquire novel or altered functions by mutation than ATs from modular PKSs.[50,51]

Material and Methods

Plasmid construction

Coding sequence for FAS and PKS constructs were cloned from genomic DNA into pET22b expression vector, performing ligation independent cloning with the In-Fusion HD Cloning Kit (Clonetech). Single point mutations were introduced in the DEBS3M5 KS^0-AT wild type gene. The sequence of all plasmids was confirmed by sequencing (Seqlab). ACP sequences were partially codon optimized for expression in *E. coli* and synthesized by Thermo Fisher. All cloning was done using *E. coli* Stellar competent cells.

Protein isolation

All constructs were expressed in *E. coli* BL21gold (DE3) cells. All ACPs were co-expressed with *Bacillus subtilis* Sfp. After induction with 0.25 mM IPTG, expression was carried out at 20 °C and 130–180 rpm overnight. Transferases were purified by tandem affinity chromatography (Ni-NTA and Strep-Tactin), ACPs were purified by Ni-affinity chromatography and size exclusion chromatography (SEC). ACP from different expression cultures was pooled after SEC. Elution fractions were analyzed by SDS-PAGE. Quality of transferases was analyzed by HPLC-SEC and thermal shift assay (TSA). Activation of ACPs was controlled by mass spectrometric analysis.

AT activity assay

The AT activity assay was adapted from references.[12,14,15] For all proteins and substrates, fresh aliquots were used. For each system, the same batch of substrates (ACP and acyl-CoAs) were used. For better comparison, for all point mutants the same batch of substrates was used. NADH fluorescence was detected in a 96-well format at fixed AT and ACP concentrations. For hydrolysis and for each ACP curve in transacylation measurements, acyl-CoA substrate concentration was varied to calculate the (apparent) K_m^{X-CoA}: (0.2; 0.3; 0.5; 0.75; 1.25; 2; 3; 5)×$K_{m(,app)}^{X-CoA}$. Fluorescence units were converted into concentrations via NADH calibration (Figure S19).

Author contributions

F.S. performed all experiments, conceived the project, analyzed data and wrote the manuscript. M.G. designed research, analyzed data and wrote the manuscript.

Acknowledgements

This project was supported by the LOEWE program (Landes-Offensive zur Entwicklung wissenschaftlich-ökonomischer Exzellenz) of the state of Hesse and was conducted within the framework of the MegaSyn Research Cluster. This project was further supported by an individual PhD scholarship from the Studienstiftung des deutschen Volkes and from the Stiftung Polytechnische Gesellschaft. We thank C. S. Heil for carefully reading and discussing the manuscript. We thank G. Grammbitter for HPLC-MS measurements and assistance with analysis of the data. We thank A. Stegemann for discussion of derivation of kinetic parameters. We thank M. Schwalm for assistance with depiction of electron density data. We thank A. Rittner for providing the plasmids pAR001, pAR090, pAR225, pAR331 and pAR333. We thank A. Fahim for performing some SEC und TSA measurements under supervision of F.S. Open access funding enabled and organized by Projekt DEAL.

Conflict of Interest

The authors declare no conflict of interest.

Keywords: Enzyme catalysis · Enzyme kinetics · Natural compound synthesis · Protein engineering · Protein-protein interactions

[1] C. S. Heil, S. S. Wehrheim, K. S. Paithankar, M. Grininger, *ChemBioChem* **2019**, *20*, 2298–2321.
[2] J. Staunton, K. J. Weissman, *Nat. Prod. Rep.* **2001**, *18*, 380–416.
[3] S. Smith, S.-C. Tsai, *Nat. Prod. Rep.* **2007**, *24*, 1041–1072.
[4] J. Beld, D. J. Lee, M. D. Burkart, *Mol. BioSyst.* **2015**, *11*, 38–59.
[5] P. Dimroth, E. Rlingelmann, F. Lynen, *Eur. J. Biochem.* **1976**, *68*, 591–596.
[6] D. A. Herbst, C. A. Townsend, T. Maier, *Nat. Prod. Rep.* **2018**, *35*, 1046–1069.
[7] T. Moriguchi, Y. Kezuka, T. Nonaka, Y. Ebizuka, I. Fujii, *J. Biol. Chem.* **2010**, *285*, 15637–15643.
[8] R. McDaniel, S. Ebert-Khosla, D. A. Hopwood, C. Khosla, *Science* **1993**, *262*, 1546–1550.
[9] J. Cortes, S. F. Haydock, G. A. Roberts, D. J. Bevitt, P. F. Leadlay, *Nature* **1990**, *348*, 176–178.
[10] L. E. Misson, J. T. Mindrebo, T. D. Davis, A. Patel, J. Andrew McCammon, J. P. Noel, M. D. Burkart, *Proc. Natl. Acad. Sci. USA* **2020**, *117*, 24224–24233.
[11] A. Miyanaga, S. Iwasawa, Y. Shinohara, F. Kudo, T. Eguchi, *Proc. Natl. Acad. Sci. USA* **2016**, *113*, 1802–1807.
[12] A. Rittner, K. S. Paithankar, K. V. Huu, M. Grininger, *ACS Chem. Biol.* **2018**, *13*, 723–732.
[13] R. A. Copeland, *Enzymes - A Practical Introduction to Structure, Mechanism, and Data Analysis*, Wiley-VCH, New York/Chichester/Weinheim/Brisbane/Singapore/Toronto **2000**, p. 355–357.
[14] J. Molnos, R. Gardiner, G. E. Dale, R. Lange, *Anal. Biochem.* **2003**, *319*, 171–176.
[15] B. J. Dunn, D. E. Cane, C. Khosla, *Biochemistry* **2013**, *52*, 1839–1841.
[16] K. J. Weissman, *Nat. Prod. Rep.* **2015**, *32*, 436–453.
[17] M. Oliynyk, M. Samborskyy, J. B. Lester, T. Mironenko, N. Scott, S. Dickens, S. F. Haydock, P. F. Leadlay, *Nat. Biotechnol.* **2007**, *25*, 447–453.
[18] T. Maier, M. Leibundgut, D. Boehringer, N. Ban, *Structure and Function of Eukaryotic Fatty Acid Synthases, Q. Rev. Biophys.* **2010**, *43*, 373–422.
[19] Y. Tang, C.-Y. Kim, I. I. Mathews, D. E. Cane, C. Khosla, *PNAS* **2006**, *103*, 11124–11129.
[20] K. Geyer, S. Sundaram, P. Sušnik, U. Koert, T. J. Erb, *ChemBioChem* **2020**, *21*, 2080–2085.
[21] S. A. Bonnett, C. M. Rath, A. R. Shareef, J. R. Joels, J. A. Chemler, K. Hkansson, K. Reynolds, D. H. Sherman, *Chem. Biol.* **2011**, *18*, 1075–1081.
[22] A. E. Szafranska, T. S. Hitchman, R. J. Cox, J. Crosby, T. J. Simpson, *Biochemistry* **2002**, *41*, 1421–1427.
[23] L. E. Misson, J. T. Mindrebo, T. D. Davis, A. Patel, J. A. McCammon, J. P. Noel, M. D. Burkart, J. Andrew, *PNAS* **2020**, *117*, 24224–24233.
[24] A. M. Marcella, A. W. Barb, *Appl. Microbiol. Biotechnol.* **2017**, *101*, 8431–8441.
[25] Y. Takamura, G. Nomura, *J. Gen. Microbiol.* **1988**, *134*, 2249–2253.
[26] M. S. Davis, J. Solbiati, J. E. Cronan, *J. Biol. Chem.* **2000**, *275*, 28593–28598.
[27] A. Fersht, *Structure and Mechanism in Protein Science. A Guide to Enzyme Catalysis and Protein*, W. H. Freeman and Company, New York **1999**.
[28] A. Bar-Even, E. Noor, Y. Savir, W. Liebermeister, D. Davidi, D. S. Tawfik, R. Milo, *Biochemistry* **2011**, *50*, 4402–4410.
[29] V. S. Rangan, S. Smith, *J. Biol. Chem.* **1996**, *271*, 31749–31755.
[30] W. J. Albery, J. R. Knowles, *Biochemistry* **1976**, *15*, 5631–5640.
[31] A. Rittner, K. S. Paithankar, A. Himmler, M. Grininger, *Protein Sci.* **2020**, *29*, 589–605.
[32] B. Lowry, T. Robbins, C. H. Weng, R. V. O'Brien, D. E. Cane, C. Khosla, *J. Am. Chem. Soc.* **2013**, *135*, 16809–16812.
[33] I. Koryakina, J. B. McArthur, M. M. Draelos, G. J. Williams, *Org. Biomol. Chem.* **2013**, *11*, 4449–4458.
[34] H. Jenke-Kodama, A. Sandmann, R. Müller, E. Dittmann, *Mol. Biol. Evol.* **2005**, *22*, 2027–2039.
[35] H. Jenke-Kodama, E. Dittmann, *Phytochemistry* **2009**, *70*, 1858–1866.
[36] A. Nivina, K. P. Yuet, J. Hsu, C. Khosla, *Chem. Rev.* **2019**, *119*, 12524–12547.
[37] B. Wang, F. Guo, C. Huang, H. Zhao, *Proc. Natl. Acad. Sci. USA* **2020**, *117*, 8449–8454.
[38] M. Grininger, *Proc. Natl. Acad. Sci. USA* **2020**, *117*, 8680–8682.
[39] E. Rossini, J. Gajewski, M. Klaus, G. Hummer, M. Grininger, *Chem. Commun.* **2018**, *54*, 11606–11609.

[40] A. Miyanaga, R. Ouchi, F. Ishikawa, E. Goto, G. Tanabe, F. Kudo, T. Eguchi, *J. Am. Chem. Soc.* **2018**, *140*, 7970–7978.
[41] M. F. Viegas, R. P. P. Neves, M. J. Ramos, P. A. Fernandes, *J. Phys. Chem. B* **2018**, *122*, 77–85.
[42] K. J. Weissman, *Nat. Prod. Rep.* **2016**, *33*, 203–230.
[43] B. J. Dunn, C. Khosla, *J. R. Soc. Interface* **2013**, *10*, 20130297.
[44] E. M. Musiol-Kroll, W. Wohlleben, *Antibiotics* **2018**, *7*, DOI 10.3390/antibiotics7030062.
[45] S. Yuzawa, K. Deng, G. Wang, E. E. K. Baidoo, T. R. Northen, P. D. Adams, L. Katz, J. D. Keasling, *ACS Synth. Biol.* **2017**, *6*, 139–147.
[46] J. Gajewski, F. Buelens, S. Serdjukow, M. Janßen, N. Cortina, H. Grubmüller, M. Grininger, *Nat. Chem. Biol.* **2017**, *13*, 363–365.
[47] M. T. Richardson, N. L. Pohl, J. T. Kealey, C. Khosla, *Metab. Eng.* **1999**, *1*, 180–187.
[48] M. Klaus, M. Grininger, *Nat. Prod. Rep.* **2018**, *35*, 1070–1081.
[49] E. Kalkreuter, J. M. Crowetipton, A. N. Lowell, D. H. Sherman, G. J. Williams, *J. Am. Chem. Soc.* **2019**, *141*, 1961–1969.
[50] R. A. Jensen, *Annu. Rev. Microbiol.* **1976**, *30*, 409–425.
[51] O. Khersonsky, D. S. Tawfik, *Annu. Rev. Biochem.* **2010**, *79*, 471–505.

Manuscript received: December 30, 2020
Revised manuscript received: February 15, 2021
Accepted manuscript online: March 4, 2021
Version of record online: March 30, 2021